Islamic Azad University
Mashhad Branch

Mineral chemistry and thermobarometry of Eocene alkaline volcanic rocks in SW Germi, NW Iran

Mohammad Mobashergarmi[1], Reza Zaraisahamia[*1], Mehraj Aghazadeh[2], Ahmad Ahmadikhalaji[1], Gholamreza Ahmadzadeh[3]

1. Department of Geology, Faculty of science, Lorestan University, Iran
2. Department of Geology, Payame Noor University, Iran
3. Department of Geology, Mohaghegh Ardabil University, Iran

Received 21 November 2016; accepted 14 August 2017

Abstract

Petrography and chemistry of minerals showing that Eocene alkaline volcanic rocks in southwestern of Germi (Talesh zone, NW Iran) mostly have basaltic composition. Mineralogically these rocks are composed of diopsidic clinopyroxene and labradoritic plagioclase phenocrysts. The microlithic and glassy groundmass composed of sanidine, clinopyroxene, biotite, pargasitic amphibole and magnetite associated with devitrified glass. Clinopyroxenes show relatively high Mg-numbers (0.76-0.93), low Al^{VI} (mostly <0.1), suggesting relatively low-pressure (~5), and water content ~2.5 to less than 10% and high oxygen fugacity (-8.38-11.51) of crystallization condition. High amount existence of magnetite coexisting with amphibole and biotite mineral confirm high fugacity of the host magma. According to clinopyroxene and feldspar thermometry, estimated crystallization temperature varies between 1106˚C to ~1200 ˚C. The clinopyroxene and amphibole mineral composition of studied rocks indicate that they have been formed in a back-arc basin environment. Mineral chemistry in the current zone shows that composition and genesis of common minerals these magmatic rocks are similar to Pushtasar basaltic rocks in the northern part of this area.

Keywords: *Mineral chemistry, Thermobarometry, Clinopyroxene, Eocene alkaline rocks, NW Iran.*

1. Introduction

Some researchers maintain that chemical composition of a mineral is related to content of the host magma and physico-chemical condition of the crystallization environment (LeBass 1962; Leterrier et al. 1982; Beccaluva et al. 1989; Abdel Rahman 1994; Molina et al. 2009). So, petrographic studies and mineral chemistry investigation are one of the best ways to identify magmatic processes. Evaluation of crystallization conditions and the processes influencing mineral crystallization could explain magmatic evolution of the host rocks accurately. Chemical composition of minerals, especially clinopyroxene, amphibole and biotite, represent valuable information about physico-chemical conditions (e.g. temperature, pressure and etc.) as well as tectonic setting of the host magma, due to they are presence in different periods crystallization of host rock (Deer et al. 1992; Molina et al. 2009).

According to a number of researchers, the composition of minerals such as pyroxene depends on the host magma (Manoli and Molin 1988; Bindi et al. 1999; Avanzinelli et al. 2004; Zhu and Ogasawara 2004). Various cations involve in the structural sites of clinopyroxene formula which are in balance with host magma (Morimoto et al. 1988), so the type and amount of cations in the various sites of general clinopyroxene formula can be used for determine the origin and evolution of host magma, magmatic series, physic-chemical condition and tectono magmatic setting of host magma (LeBass 1962; Leterrier et al. 1982; Morimoto et al. 1988; Beccaluva et al. 1989; Bindi et al. 1999; Avanzinelli et al. 2004).

Ca-rich clinopyroxene crystals are one of the most common ferromagnesian minerals in sodic and potassic alkaline rocks from various tectonic settings. The occurrence of Ca-rich clinopyroxene phenocrysts in alkaline volcanic rocks from collision zone or post-collision setting has been generally considered to provide important clues to the nature of crystallization and evolution of related magma (Avanzinelli et al. 2004). According to chemical composition and cation replacement in crystalline sites of clinopyroxene minerals, physico-chemical condition of host magma (e.g. temperature, pressure and fugacity) during crystallization of clinopyroxene can be measured (Schweitzer et al. 1979). So different studies have been demonstrated that composition of pyroxene can be used to determine of physico-chemical condition of host magma such as pressure and fugacity, and so a formula for measuring temperature of crystallization of clinopyroxene crystals have been developed (Taylor and Nimis 2000). As well phyllosilicate minerals are influenced by chemistry of host magma (Beane 1974), and they are used for determining magmatic nature, oxygen fugacity and thermometry of host magma.

*Corresponding author.
E-mail address (es): Zareisah@yahoo.com

Amphiboles are considered as common components of igneous rocks and formed in wide ranges of temperature and pressure (Hammarstrom and Zen 1986). Chemical compositions of amphiboles have strong correlation with magmatic evolution and crystallization of the host rocks so that we can evaluate geochemical properties and tectonic environment of the host. Wide chemical formula of amphiboles cause large number of captions enter in the crystalline structure and content of some cations such as Na, Ca, Ti, Al depend on pressure, temperature and oxygen fugacity that these cations can be used thermobarometry calculations of amphibole (Hammarstrom and Zen 1986). Due to buffer of crystalline system of amphibole, Ti and Al contents in the tetrahedral position reflect thermobarometric conditions (Wones and Gilbert 1982: Hendry et al. 1985; Hammarstrom and Zen 1986; Vynhal et al. 1991; Stein and Dietl 2001). Also in structural formula of amphiboles, the Al^{VI} to Al^{Total} ratio is a basic parameter to measure of pressure, which changes according to pressure in a linear form (Schmidt 1992). According to Yoder et al (1962), crystallization temperature of feldspars can be measured by determining values of albite, anorthite and *sanidine* existing in the composition of them as solid dissolution (Perugini et al. 2005; Gioncada et al. 2006).

There are some outcrops of Eocene volcanic rocks in southwestern of Germi city (Fig 1). This area is a part of Talesh zone and Alborz-Azarbaijan volcanic belt (Berberian and Berberian 1981; Aghazadeh et al. 2010, 2011; Castro et al. 2013; Masson et al. 2006).

Mobashergermi et al. (2015) have already conducted studies to evaluate the petrography and mineral chemistry of basaltic prisms in southwest of Germi city (South talesh) whereas the area of this research is known as Pushtasar basaltic rocks (Unit E^{ba}). These basaltic rocks are mostly prismatic structure with base of pillow lava structure (Mobashergermi et al, 2013). The other previous study conducted in this area entitled: geochemistry, petrogeneses and origin magmatic evolution in the olivine gabbros of southwest of Germi city (Mobashergermi et al. 2015) on the northern of this area (Unit E^{g}) (Fig 1).

According to Mobashergermi et al (2015), the Pushtasar basaltic prisms assemblages in south-eastern of Germi are contain of Eocene mafic volcanic rocks such as olivine basalt. They have been outcropped with about 1000 meters thickness in eastern part to 10 meters thickness in western part of Moghan area. The main minerals of these basalts are olivine phenocrysts, clinopyroxene (Augite to diopside) and labradoritic plagioclase. The dominant textures of these rocks are microlitic porphyritic. Pushtasar basaltic rocks, According to whole rocks and mineral chemistry data are originated from an alkaline magma and also whole rocks geochemistry show the parent magma has been enriched source. In the following an association of olivine-gabbroic rocks with mineralogy consists of phenocrysts of plagioclase, clinopyroxene (Augite to diopside), and olivine with a lesser amount minerals of biotite, amphibole, apatite, opaque and zircon. The dominant textures in these rocks are granular and ophitic. From the whole rock chemical aspect, generating magma in these rocks is alkaline with high richness in LREE which is related to enriched mantle and indicates evolution process through differentiation. The olivine gabbros are formed from an extensional back arc basin resulting from subduction related to Neothetyse (Mobashergermi et al. 2015). The aims of this study are petrography and mineral chemistry of mentioned volcanic rocks (Unit E^{b}) and use of chemistry of minerals (e.g. clinopyroxene, feldspars, biotite and amphibole) to determine physico-chemical condition of host magma. In addition, we will try to determine nature of magma and tectono-magmatic setting of the host magma by using mineral chemistry.

2. Geological setting

The study area is located in coordinate 47° 32′ to 48° 00′ E longitudes and 38° 59′ to 39° 50′ N latitudes in the Southwest of Germi, NW Iran. Based on Iranian tectono- structural divisions, studied area is part of the Alborz-Azerbaijan magmatic belt and Talesh sub-zone (Babakhani and Khan Nazer 1997; Brunet et al. 2003) (Fig 1). Geologically, studied area composed of Cretaceous, Paleocene and Eocene volcanic and sedimentary rocks (Fig 1) with oldest outcrops include Cretaceous volcanic rocks. These volcanic rocks disconformity overly by Paleocene flysch type deposits including more than 5000m detrital deposits. The Paleocene flysch type deposits mainly consist of shale, siltstone, limy sandstone, tuffaceous sandstone, sandstone and conglomerate. The Paleocene deposit has been covered by Eocene thick sedimentary strata including conglomerate, tuffaceous sandstone and sandstone. This stratum in the upper part includes layers of tuff and sandy tuff. Conglomerate of this unit includes fragments of various volcanic rocks, limestone, and radiolarian chert. In the upper parts of the Eocene sedimentary unit, there are layers of volcanic rocks with different thickness. Lower discontinuous layer including analcime phenocrysts with thickness about 1-2 m. Upper layer show more than 300m thick and include columnar jointing and pillow structures. Upper layer volcanic rocks have porphyry texture with feldspar and mafic mineral phenocrysts. The layer, especially in the lower and middle parts, includes amygdales that have been filled by calcite, silica and chlorite. It is deduced that they are generated in a shallow marine setting. The upper volcanic layer covered by Eocene flysch type deposits including shale, marl, sandstone and conglomerate that these units belong to Moghan depression system.

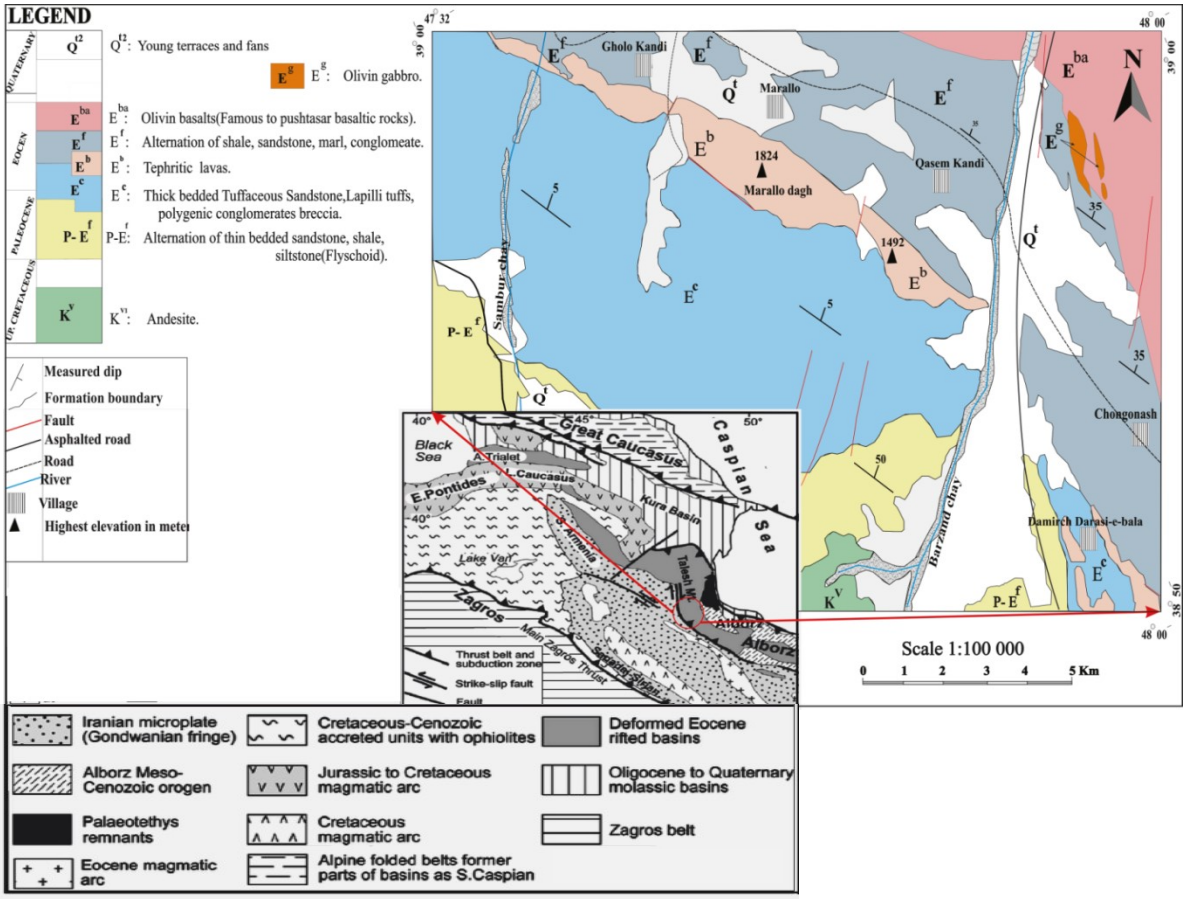

Fig 1. Geological map of study area southwest of Germi, demonstrated partial of Lahrud Geological map on the scale of 1:100,000 (Babakhani and Khan Nazer 1997) with field corrections respect to Talesh zone (Brunet et al. 2003).(The studied Basalt is show with the E^b symbol)

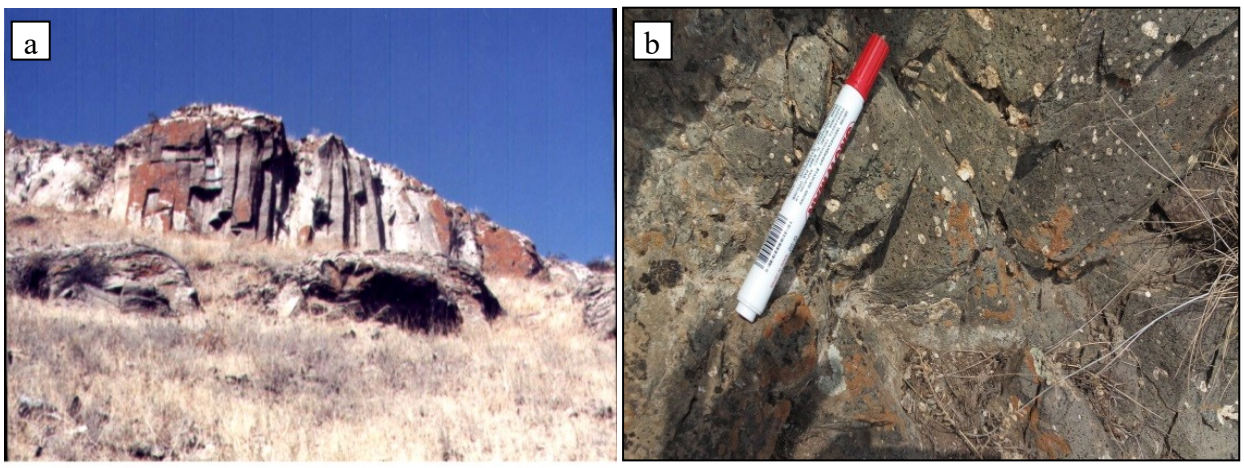

Fig 2. a) A view of basaltic prisms looking NE. b) Amygdales occurred in the basaltic prisms in the study area.

3. Analytical Methods

Volcanic layers have been studied in detail during field surveying and several samples have been gathered. Thirty samples sent to lab and thin sections have been were prepared. Thin sections were studied in detail by plan-polarized microscope the OlympusBH2 at the Lorestan University. Then five thin sections selected for EPMA analysis and they analyzed in by using

CAMECA-SX-100 instrument whit wavelength 5 Mm dispersive system (WDS) combined with operating conditions of 15 Kev, 0.2 microamperes beam current and a beam diameter of about 5 microns at the mineralogical lab of Iranian Mines & Mining Industries Development and Renovation Organization. Several spots from different clinopyroxene and plagioclase crystals have been analyzed. The results of analyzed spots were listed in Table (1, 2 and 3). Clinopyroxenes have been measured according to six oxygen while plagioclase resulted on basis of eight oxygen. Also, opaque mineral, biotite, amphibole and alkali feldspar measured according to 3, 22, 23 and 8 oxygen respectively.

4. Petrography

Outcrops of volcanic rocks in the southwest of Germi show dark grey to black colour. They have porphyry, glomeroporphyritic (Fig 3a) and hyalomicroporphyritic textures with clinopyroxene phenocrysts (Fig 3b). Clinopyroxene minerals occur as large (up to 4 mm) isolated phenocrysts types which have subhedral to euhedral shape and are mostly fresh. Generally, it can be stated that frequency of clinopyroxene minerals are more than 30% modal volume. Some clinopyroxene minerals include crystals of opaque minerals as poikilitic Texture, which indicates, syn crystallization of both crystals (Fig 3a, b). Some clinopyroxene crystals show sieve texture and compositional zoning. Development of both normal and sieve-textured clinopyroxenes can just be resulted from decreasing pressure; however, crystallization from hydrous melt may lead to such textures (Kuscu and Floyd 2001). Some clinopyroxene crystals show oscillatory normal zoning (Fig 3c). Microlithic groundmass of these rocks includes alkali feldspars, mica, opaque minerals and volcanic glass (Fig 3d). In the groundmass, alkali feldspars are sanidine crystals (Fig 3a, b and d). Plagioclase crystals are often fresh and euhedral with size over >0.5 mm and almost show polysynthetic twining (Fig 3d).

The studied basalt mostly consists of pyroxene and plagioclase phenocrysts in a groundmass of microlithic crystals as well as opaque minerals, alkali feldspar, brown needle microcrystals and glass. Brown needle microcrystals based on EPMA analysis are biotite and amphibole. In some cases, brown biotitic and amphibole micro crystals (with less than 5% modal volume frequency) have been alterated to Chlorite (Fig 3d).

The opaque minerals mostly show less than 10% frequency. They represent as both microphenocryst and microcrystal in the groundmass, and even in the form of inclusions inside clinopyroxene phenocrysts (Fig 3a, b and d). The biotite and amphibole minerals are observed generally as needle form and very fine-grained with the size less than 15 microns. In the groundmass of the studied rocks, there are some sanidines crystals that are common in the sample which have been gathered from center of volcanic layer. Existence of amphibole and biotite associated with sanidine in the matrix of the studied rocks implies being more potassium-rich rocks.

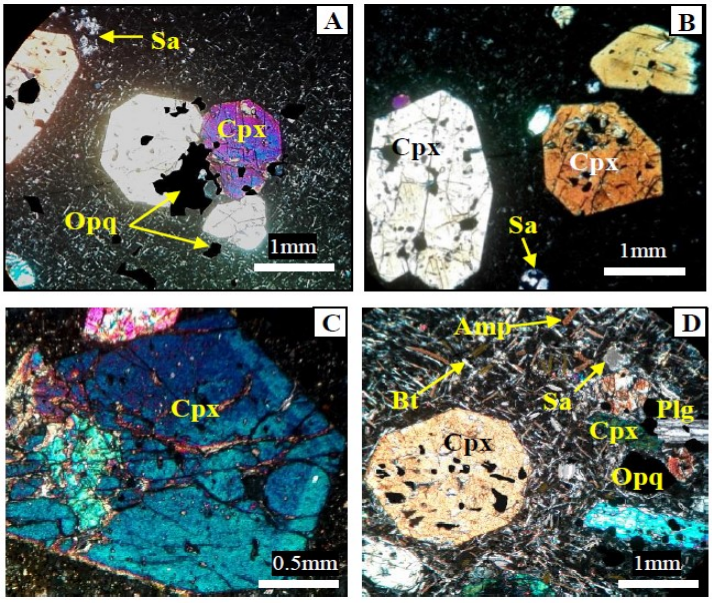

Fig 3. a) Glomeroporphyritic texture in the studied basalts (XPL). b) Hyalomicroporphyritic texture demonstrate Clinopyroxene phenocrysts in a glassy matrix (XPL). c) Normal zoning type of clinopyroxenes in the studied alkaline basalt rocks located in the southwest of Germi. d) This figure shows phenocrysts clinopyroxenes minerals, opaque minerals and plagioclase minerals with microliths of amphibole, biotite and sanidine in the basalts of southwest Germi (XPL). Abbreviations for names of minerals are derived from Whitney and Evans (2010).

5. Mineral chemistry

Several crystals from different minerals have been analyzed by EPMA. Plagioclase crystals are mostly of calcic type and their anorthite components vary between 50.2% to 69.4% (Labradorite) (Table 1). Their plagioclase contents vary between 29-49% volumes, also orthoclase component between 0.3-5.4 percent, (Fig 4a). Thus they do not show chemical zoning. According to EPMA data contain from three feldspars microcrystal of groundmass, they have contain sanidine composition and major oxides of the crystals that represent limited changes as SiO_2 (63.21- 63.37) (wt.%), CaO (1.81-2.10) (wt.%), Na_2O (0.69-0.74) (wt.%), K_2O(14.71-14.88) (wt.%) and Al_2O_3 (17.11-17.13) (wt.%) with $Or_{83.68}$ - $Or_{85.13}$ (Table 1) In the feldspar classification diagram (Fig 4a) studied crystals are placed in the field of sanidine.

Clinopyroxene is one of the most abundant mineral in the studied mafic-alkaline rocks. Major given representative element compositions and site occupancies of the investigated clinopyroxenes are presented in Table (2). Clinopyroxene crystals generally have high Mg#= [Mg/ ($Mg+Fe^{2+}$)] of 0.76–0.93, variable Al_2O_3 (2.94–5.46 wt. %), TiO_2 0.52-0.98 wt. %) and Na_2O (0.54-0.69 wt. %) contents. Clinopyroxene minerals have Wo (45-50), En (40 - 47), Fs (0.5-15) (Table 2) and all analysed spots are placed in the diopside filed of Wo-En-Fs diagram (Deer et al. 1992) (Fig 4b).

Table 1. Represent calculated mineral formulas of plagioclase and groundmass microlithic alkali feldspars (Based on 8 oxygen) minerals in the basaltic rocks in Southwest of Germi.

Plg	10/1.	12/1.	11 / 1.	7 / 1.	6 / 1.	5 / 1.	A/1	A/2	A/3	Kf	10/2.m	10/12.m	10/19.m
SiO_2	52.62	53.42	55.48	50.89	51.46	55.75	51.96	52.01	52.38	SiO_2	63.21	63.26	63.37
TiO_2	0.68	0.01	0.04	0.02	0.04	0	0.59	0.54	0.31	TiO_2	0.11	0.09	0.09
Al_2O_3	28.42	28.82	29.5	30.68	29.9	25.97	28.44	28.46	28.58	Al_2O_3	17.13	17.13	17.11
FeO	1.42	0.75	0.57	0.42	0.28	0.18	1.41	1.12	0.99	FeO	0.68	0.48	0.59
MnO	0.05	0.03	0	0	0	0.04	0.05	0.03	0.02	MnO	0.05	0	0
MgO	0.52	0.12	0.13	0.01	0	0	0.41	0.35	0.33	MgO	0.43	0.41	0.41
CaO	12.33	11.85	10.65	12.72	12.45	10.44	12.3	12.11	11.91	CaO	2.1	1.92	1.81
Na_2O	2.96	2.91	3.48	3.97	4.28	5.68	2.91	2.89	2.88	Na_2O	0.74	0.71	0.69
K_2O	0.06	0.48	0.18	0.09	0.13	0.06	0.31	0.79	0.82	K_2O	14.81	14.88	14.71
Total	99.06	98.39	100.03	98.8	98.54	98.12	98.38	98.3	98.22	Total	99.26	98.88	98.78
Oxygen's	8	8	8	8	8	8	8	8	8	Oxygen's	8	8	8
Si	2.41	2.45	2.48	2.34	2.37	2.56	2.4	2.41	2.42	Si	2.97	2.97	2.98
Al	1.54	1.56	1.56	1.66	1.62	1.41	1.55	1.55	1.56	Al	0.95	0.95	0.95
Ti	0.02	0	0	0	0	0	0.02	0.02	0.01	Ti	0	0	0
Fe	0.05	0.03	0.02	0.02	0.01	0.01	0.05	0.04	0.04	Fe	0.03	0.02	0.02
Mg	0.04	0.01	0.01	0	0	0	0.03	0.02	0.02	Mg	0.03	0.03	0.03
Ca	0.61	0.58	0.51	0.63	0.62	0.51	0.61	0.6	0.59	Ca	0.11	0.1	0.09
Na	0.26	0.26	0.3	0.35	0.38	0.51	0.26	0.26	0.26	Na	0.07	0.06	0.06
K	0	0.03	0.01	0.01	0.01	0	0.02	0.05	0.05	K	0.89	0.89	0.88
Total	4.93	4.92	4.89	5.01	5.01	4.99	4.94	4.95	4.94	Total	5.03	5.03	5.02
Or	0.4	3.2	1.2	0.5	0.8	0.3	2.1	5.1	5.4	Or	83.68	84.68	85.13
Ab	30	30	37	36	38	49	29	29	29	Ab	6.36	6.14	6.07
An	69.4	67	62.1	63.6	61.2	50.2	68.6	66.2	65.8	An	9.97	9.18	8.8
log fO_2 (France et al. 2010)		-8.5	-8.38	-8.8	-8.97	-9.77	-10.57	-11.5					

In the Ti–Na- Al^{IV} triangular diagram of Papike et al (1976) the compositions of most of clinopyroxenes fall in the Ca-Tschermark's (CATS) field (Fig 4d). The studied clinopyroxenes show variable Al (a.p.f.u) 0.13-0.24 and Fe^{3+} (a.p.f.u) 0.04 -0.16 contents, and in the diagram Al (a.p.f.u) vs. Fe^{3+} (a.p.f.u) of (Morimoto et al. 1988), clinopyroxenes diagram located in the Aluminium – Aluminium ferrian diopside field (Fig 4e). According to two electron probe micro analyses (EPMA) analysis of biotite from groundmass microcrystals the major oxides are varies as FeO (14.56-16.32) (wt. %), MgO (12.06-14.47) (wt.%) and Al_2O_3 (15.53- 16.56) (wt. %) (Table 3).

Also According to the Q ($Ca+Mg+Fe^{2+}$) vs. J (2Na) classification diagram (Deer et al. 1992) all the analysed clinopyroxenes fall in the region of iron magnesium and calcium clinopyroxenes (Fig 4c). This study shows the similarity of chemistry composition of minerals among this basaltic rocks and Pushtasar basaltic prisms rocks in the northern part of this area. Pushtasar basaltic rocks have composition of plagioclase whit amounts An (55-57) are labradoritic and clinopyroxenes with amounts of Wo (39-43), Fs (14-18) and En (40-44) are diopside to augite containing Fe-Mg-Ca which shown on figures (4 a, b and c) (Mobashergermi 2013; Mobashergermi et al. 2015). According to mica classification diagram (Deer et al. 1992), analyzed crystals show biotitic composition with Fe/ (Fe+Mg)>0.33. Studied crystals show biotite composition in the diagram Al_{Total} vs. Fe# (Fig 4f), and the range of end members in the diagram varies between Fe# (0.39- 0.40) and Al_{Total} (2.73-2.96) (a.p.f.u).

Table 2. Represent calculated mineral formulas of clinopyroxene minerals in the basaltic rocks in southwest of Germi (Based on 6 oxygen).

Cpx	Core 3 / 1.	Rim 4 / 1.	Core 14 / 1.	Rim 13 / 1.	Core 18 / 1.	Core 17 / 1.	Core 16 / 1.	Rim 15 / 1.	Core 2 / 1.	Rim 1 / 1.	Core 4 / 1.	Rim 3 / 1.	Core A/1	Rim A/2	Core 1 / 1.	Rim 2 / 1.
SiO_2	50.2	50.31	50.46	50.78	48.96	49.07	49.63	50.12	50.5	50.74	49.43	50.31	50.09	50.14	49.87	49.97
TiO_2	0.72	0.65	0.62	0.52	0.76	0.73	0.73	0.69	0.67	0.6	0.75	0.74	0.61	0.57	0.98	0.78
Al_2O_3	3.14	3.16	3.85	2.94	4.75	5.04	5.36	5.46	3.09	4.11	4.01	5.22	4.99	5.09	5.02	5.13
Cr_2O_3	0	0	0.38	0.3	0.02	0.03	0.06	0.1	0.1	0.01	0.1	0.1	0.01	0.01	0	0.01
FeO	8.57	8.21	6.09	6.35	7.86	7.89	7.78	7.98	8.42	8.46	8.03	8.88	7.76	7.94	7.77	9.11
MnO	0.34	0.33	0.23	0.24	0.29	0.26	0.24	0.24	0.4	0.31	0.35	0.32	0.28	0.24	0.29	0.31
MgO	14.17	14.1	15.8	15.46	14.11	13.54	13.42	13.36	14.04	13.91	13.93	13.32	14.09	13.99	13.74	13.02
CaO	22.48	21.8	22.66	22.46	22.2	21.72	22.12	22.03	20.73	21.03	21.2	21.02	21.8	21.24	22.39	21.15
Na_2O	0.6	0.62	0.54	0.45	0.54	0.55	0.53	0.52	0.63	0.55	0.69	0.51	0.62	0.61	0.52	0.69
Total	100.22	99.18	100.64	99.5	99.49	98.83	99.88	100.5	98.58	99.72	98.49	100.42	100.25	99.84	100.59	100.17
Si	1.86	1.88	1.84	1.88	1.82	1.84	1.84	1.85	1.9	1.89	1.85	1.86	1.84	1.85	1.83	1.85
Ti	0.02	0.02	0.02	0.01	0.02	0.02	0.02	0.02	0.02	0.02	0.02	0.02	0.02	0.02	0.03	0.02
Al	0.14	0.14	0.17	0.13	0.21	0.22	0.23	0.24	0.14	0.18	0.18	0.23	0.22	0.22	0.22	0.22
Fe(III)	0.16	0.12	0.16	0.1	0.16	0.1	0.09	0.07	0.07	0.05	0.12	0.04	0.11	0.08	0.1	0.08
Fe(II)	0.11	0.14	0.03	0.09	0.09	0.14	0.16	0.18	0.19	0.21	0.13	0.23	0.13	0.16	0.14	0.21
Mn	0.01	0.01	0.01	0.01	0.01	0.01	0.01	0.01	0.01	0.01	0.01	0.01	0.01	0.01	0.01	0.01
Mg	0.78	0.78	0.86	0.85	0.78	0.76	0.74	0.73	0.79	0.77	0.78	0.73	0.77	0.77	0.75	0.72
Ca	0.89	0.87	0.88	0.89	0.88	0.87	0.88	0.87	0.83	0.84	0.85	0.83	0.86	0.84	0.88	0.84
Na	0.04	0.05	0.04	0.03	0.04	0.04	0.04	0.04	0.05	0.04	0.05	0.04	0.04	0.04	0.04	0.05
K	0	0	0	0	0	0	0	0	0	0	0	0	0	0	0	0
Total	4.01	4	4	4	4	4	4	4	4	4	4	4	4	4	4	4
Site T																
Si	1.86	1.88	1.84	1.88	1.82	1.84	1.84	1.85	1.9	1.89	1.85	1.86	1.84	1.85	1.83	1.85
Al^{IV}	0.14	0.12	0.16	0.12	0.18	0.16	0.16	0.15	0.1	0.11	0.15	0.14	0.16	0.15	0.17	0.15
Total SiteT	2	2	2	2	2	2	2	2	2	2	2	2	2	2	2	2
Site M_1																
Al^{VI}	0	0.01	0	0.01	0.02	0.06	0.07	0.08	0.03	0.07	0.03	0.09	0.06	0.08	0.05	0.08
Fe(III)	0.16	0.12	0.16	0.1	0.16	0.1	0.09	0.07	0.07	0.05	0.12	0.04	0.11	0.08	0.1	0.08
Ti	0.02	0.02	0.02	0.01	0.02	0.02	0.02	0.02	0.02	0.02	0.02	0.02	0.02	0.02	0.03	0.02
Fe(II)	0.11	0.14	0.03	0.09	0.09	0.14	0.16	0.18	0.19	0.21	0.13	0.23	0.13	0.16	0.14	0.21
Mg	0.72	0.71	0.79	0.77	0.71	0.67	0.67	0.65	0.68	0.65	0.69	0.61	0.69	0.66	0.68	0.62
Total Site M_1	1	1	1	1	1	1	1	1	1	1	1	1	1	1	1	1
Site M_2																
Fe(II)	0	0	0	0	0	0	0	0	0	0	0	0	0	0	0	0
Mg	0.06	0.07	0.07	0.08	0.07	0.08	0.08	0.09	0.11	0.12	0.09	0.12	0.09	0.11	0.07	0.1
Ca	0.89	0.87	0.88	0.89	0.88	0.87	0.88	0.87	0.83	0.84	0.85	0.83	0.86	0.84	0.88	0.84
Na	0.04	0.05	0.04	0.03	0.04	0.04	0.04	0.04	0.05	0.04	0.05	0.04	0.04	0.04	0.04	0.05
Mn	0.01	0.01	0.01	0.01	0.01	0.01	0.01	0.01	0.01	0.01	0.01	0.01	0.01	0.01	0.01	0.01
Total Site M_2	1	1	1	1	1	1	1	1	1	1	1	1	1	1	1	1
En	0.43	0.43	0.47	0.45	0.43	0.43	0.42	0.43	0.43	0.42	0.44	0.4	0.44	0.43	0.42	0.41
Fs	0.08	0.1	0.05	0.08	0.06	0.08	0.09	0.08	0.11	0.12	0.08	0.15	0.07	0.09	0.08	0.12
Wo	0.49	0.48	0.48	0.47	0.5	0.49	0.49	0.49	0.46	0.46	0.48	0.45	0.49	0.47	0.5	0.48
$Mg/(Mg+Fe^{2+})$	0.88	0.85	0.97	0.9	0.9	0.84	0.83	0.8	0.8	0.78	0.85	0.76	0.86	0.83	0.84	0.78
Fe^{2+}/Fe^{total}	0.41	0.54	0.15	0.48	0.36	0.58	0.64	0.73	0.72	0.81	0.53	0.84	0.55	0.66	0.59	0.73
$Al/(Al+Fe^{3+}+Cr)$	0.47	0.54	0.5	0.54	0.57	0.68	0.73	0.78	0.64	0.78	0.59	0.83	0.67	0.73	0.69	0.74
Ca+Na	0.93	0.92	0.92	0.92	0.92	0.91	0.92	0.91	0.88	0.88	0.9	0.87	0.9	0.89	0.92	0.89
$Al^{IV}+Na$	0.19	0.17	0.2	0.15	0.22	0.2	0.2	0.19	0.15	0.15	0.2	0.18	0.2	0.19	0.2	0.2
$Al^{VI}+2Ti+Cr$	0.04	0.05	0.05	0.05	0.07	0.1	0.11	0.13	0.08	0.1	0.08	0.13	0.09	0.11	0.11	0.12
J	0.09	0.09	0.08	0.06	0.08	0.08	0.08	0.07	0.09	0.08	0.1	0.07	0.09	0.09	0.07	0.1
Q	1.78	1.79	1.77	1.83	1.75	1.77	1.77	1.78	1.81	1.82	1.76	1.8	1.76	1.77	1.78	1.77
Ti+Cr	0.02	0.02	0.03	0.02	0.02	0.02	0.02	0.02	0.02	0.02	0.02	0.02	0.02	0.02	0.03	0.02
T(C°)*	1197	1204	1241	1241	1205	1204	1208	1208	1198	1203	1201	1190	1215	1213	1198	1185
Ti+Cr+Na	0.06	0.06	0.07	0.06	0.06	0.06	0.06	0.06	0.07	0.06	0.07	0.06	0.06	0.06	0.06	0.07
Al^{VI}/Al^{IV}	0.02	0.12	0.01	0.09	0.13	0.35	0.44	0.55	0.33	0.61	0.21	0.64	0.38	0.51	0.31	0.51
$TiO_2+Cr_2O_3$	0.72	0.65	1	0.82	0.78	0.76	0.79	0.79	0.77	0.61	0.85	0.84	0.62	0.58	0.98	0.79
T°C **	1067	1115	1212	1117	1128	1105	1063	1067	1197	1167	1196	1145	1171	1202	1064	1142
TCpx***	1032	1083	1053	1048	1056	1083	1066	1085	1159	1157	1124	1161	1109	1146	1056	1148
XpT	38	38	38	38	36	36	36	36	37	37	36	36	37	36	37	36
YpT	-27	-28	-30	-29	-28	-27	-28	-28	-27	-28	-27	-27	-28	-28	-28	-27

** (Taylor and Nimis 2000)* ***(Kretz 1994)* ****(Bertrand and Mercier 1985)*

Major elements from two analysis of amphibole microcrystals from groundmass of the studied volcanic rocks varies as SiO_2 (43.60-45.16) (wt. %), MgO (7.72-8.71) (wt. %), Al_2O_3 (17.18-18.24) (wt. %) and K_2O (7.83-8.86) (wt. %) (Table 3). Amphibole microcrystal with Si (6.42-6.61) (a.p.f.u) and Mg# (0.53-0.59) (a.p.f.u) contents shows pargasitic composition in the diagram TSi (a.p.f.u) vs. Mg# (Fig 5a).

Magnetite analyzed crystals structural formula is calculated based on 3 oxygen (Deer et al. 1992). Magnetite crystals generally show FeO> 70(wt. %), TiO_2< 8(wt. %) contents (Table 3), and Ti and Fe contents varies between 2.03- 2.12 and 0.13-0.19 respectively, in the basaltic rock in southwest of Germi area.

Table 3. Demonstrates the calculated mineral formulas of microlithic biotite minerals in groundmass (Based on 22 oxygen), microlithic amphibole minerals formulas (Based on 23 oxygen) and magnetite formulas (Based on 3 oxygen) in the basaltic rocks of southwestern Germi.

Bt	7/1.m	9/1.m	Am	8/1.m	9/1. m
SiO_2	35.68	36.44	SiO_2	43.6	45.16
TiO_2	1.78	1.94	TiO_2	1.02	1.34
Al_2O_3	16.56	15.53	Al_2O_3	18.24	17.18
FeO	14.56	16.32	FeO	12.58	11.66
MnO	0.3	0.39	MnO	7.72	8.71
MgO	12.06	14.47	MgO	0.34	0.3
CaO	2.75	1.71	CaO	3.59	1.28
Na_2O	1.57	0.6	Na_2O	1.67	1.12
K_2O	8.98	7.11	K_2O	7.83	8.86
Total	94.24	94.51	Total	96.59	95.61
Oxygen's	22	22	Oxygen's	23	23
Si	5.4	5.43	T-sites Si	6.42	6.61
Al^{IV}	2.6	2.57	T-sites Al^{IV}	1.58	1.39
Al^{VI}	0.36	0.16	C- sites Al^{VI}	1.59	1.58
Ti	0.2	0.22	C- sites Ti	0.11	0.15
Fe	1.84	2.03	C- sites Fe^{3+}	0.02	0.02
Mn	0.04	0.05	C- sites Mg	1.7	1.9
Mg	2.72	3.22	C- sites Mn	0.04	0.04
Ca	0.45	0.27	C- sites Fe^{2+}	1.53	1.32
Na	0.46	0.17	C- sites Ca	0.01	0
K	1.73	1.35	B- site Fe^{3+}	0	0.093
OH*	4	4	B- site Ca	0.56	0.2
Total	13.16	13.68	B- site Na	1.44	1.71
Y total	5.58	6.22	A- site Na	0	0
X_{total}	2.64	1.8	A- site K	1.47	1.66
Al_{total}	2.96	2.73	Sum cations	16.47	16.66
Fe#	0.4	0.39	$Fe^{3+}/(Fe^{3+}+Al^{VI})$	0.01	0.07
Total Al	2.96	2.73	Al^{total}	3.17	2.97

Mag	11 / 1.	5 / 1.	6 / 1.	1/1.	1/2.
SiO_2	0.25	0.22	0.14	0.29	0.18
TiO_2	5.28	7.44	5.23	6.28	7.24
Al_2O_3	6.59	5.04	7.53	6.95	7.54
FeO	76.73	75.69	76.78	77.21	77.83
MnO	0.57	0.58	0.51	0.51	0.53
MgO	4.8	3.4	4.9	3.2	4.1
CaO	0.03	0.06	0.06	0.04	0.05
Na_2O	0.06	0.09	0	0.03	0.08
Total	94.31	92.52	95.15	94.51	97.55
Oxygen's	3	3	3	3	3
Si	0.01	0.01	0	0.01	0.01
Al	0.25	0.2	0.29	0.27	0.28
Ti	0.13	0.19	0.13	0.15	0.17
Fe	2.09	2.12	2.06	2.1	2.03
Mn	0.02	0.02	0.01	0.01	0.01
Mg	0.23	0.17	0.23	0.16	0.19
Ca	0	0	0	0	0
Na	0	0.01	0	0	0.01
minerals	Magnetite	Magnetite	Magnetite	Magnetite	Magnetite

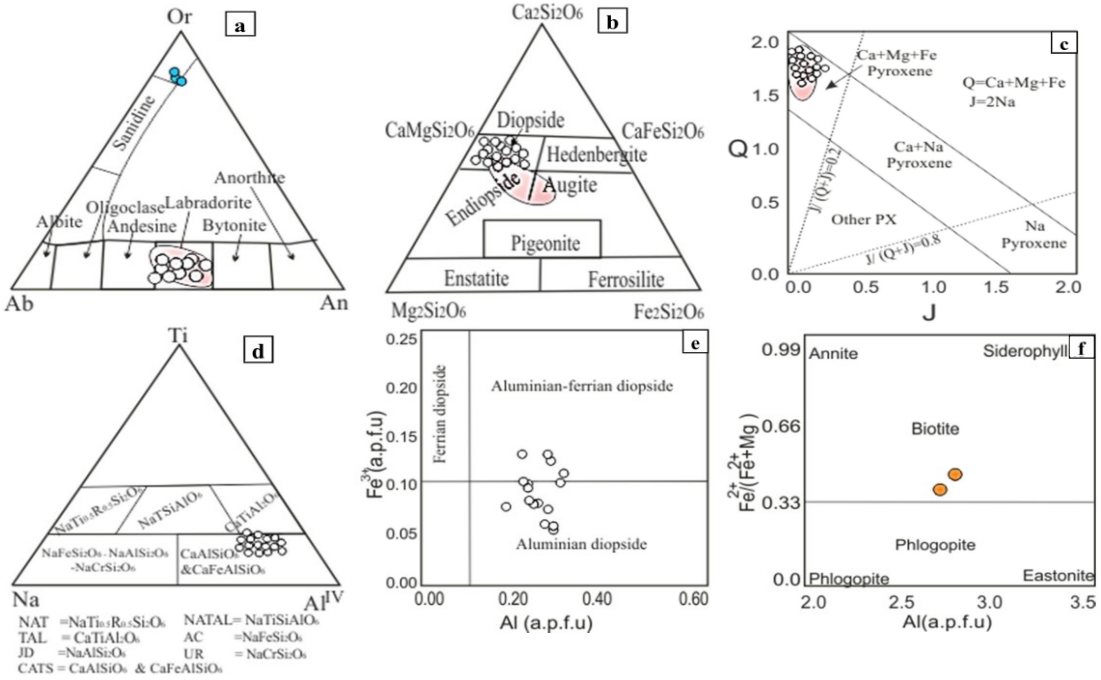

Fig 4. a)Triangular classification diagram (Deer et al. 1992) all phenocrysts feldspars are labradorite in composition and microlithic groundmass feldspars show sanidine composition from basaltic rocks in Southwest of Germi. b) Clinopyroxenes classification diagram after Deer et al. (1992), all composition of clinopyroxenes are diopside. c) The Q-J clinopyroxene classification diagram after Morimoto et al. (1988). All clinopyroxenes are in the Q (Ca+Mg+Fe) field. [The range determined in the diagrams (Fig 4a, b, and c) is relevant to mineral chemistry in the Pushtasar basaltic rocks (Mobashergermi et al. 2015). d) The Ti–Na- Al^{IV} triangular diagram (Papike et al. 1974), most of clinopyroxenes are in the Ca-Tschermark's molecule (CATS) field. e) The Al (a.p.f.u) versus Fe^{3+} (a.p.f.u) diagram of (Morimoto et al. 1988) shows all the samples are Aluminian – Aluminian ferrian diopside. f) In the diagram of chemical classification of micas (Deer et al. 1992), all mica microcrystal samples are in the range of biotites.

6. Thermobarometry

Experimental studies indicate that mineral compositions can be effectively used to quantify the P-T conditions during crystallization (Berman 1988; Gasparik 1984). In order to determine the temperature and pressure formation of the studied basaltic rocks, clinopyroxene barometry and thermometry has been used. Analysed clinopyroxenes crystals are situated around 1200 ˚C in thermometry diagram of Soesoo (1997) (Fig 5b). Considering thermometry of (1) Taylor and Nimis (2000), (2) Kretz (1994), (3) Bertrand and Mercier (1985), estimated temperatures are varies between 1185 to 1241˚C, 1063 to 2012 ˚C and 1059 to 1148˚C, respectively for basaltic rocks in the southwest of Germi (Table 2). All different thermometries are match together.

(1) $T^{\circ C}$ *(Cpx) = ([23166+39.28P (kbar)] / [13.25 + 15.35Ti + 4.5Fe- 1.55(Al+Cr-Na) + (Ln*a_{en}^{Cpx}*)*^{2}*] ±25*$^{C^\circ}$*)-274*

a_{en}^{Cpx} *= (1–Ca–Na–K) (1–1/2(Al+Cr+Na+K)*

(2) $T^{\circ C}$ *(Cpx) = {1000/ (0.054+0.608XCpx-0.304Ln (1- 2[Ca] Cpx))}-273*

X_{Cpx} *= [*Fe^{2+}*/ (*Fe^{2+}*+Mg)]* $_{Cpx}$

(3)$T^{\circ C}$ *(Cpx) = (33696+45.45P)/ (17.61-8.314Ln [(1-* X^{M2}_{Ca}*)/0.95]-12.13[*X^{M2}_{Ca}*]* ^{2}

The plagioclase crystals thermometry represent 950 to higher than 1000 ˚C-temperature according to diagram of Kroll et al. (1993) (Fig 5c). Sanidine crystals in groundmass mostly are fields in the temperature range 900 to 1000 $^{\circ C}$. The diagram can have up to ±50$^{\circ C}$ error (Kroll et al. 1993). According to the low- moderate Al^{VI} (0.00 - 0.09), Al^{IV} (0.10-0.18) and Al^{VI}/Al^{IV} (0.01-0.6) ratio contents of studied clinopyroxenes, they have been crystallized in a low-pressure condition (Aoki and Shiba 1973). Also, in the Al^{VI} versus Al^{IV} diagram (Helz 1976); all analyzed pyroxenes of the studied rocks are located in the low-pressure field (Fig 5d). The content of Al in clinopyroxene crystals has been used to determine the depth of the magma chamber (Aoki and Shiba 1973). According to diagrams Al^{IV} versus Al^{VI} (Aoki and Shiba 1973), the studied clinopyroxenes crystallized at water content of ~2.5 to less than 10% (Fig 5e).

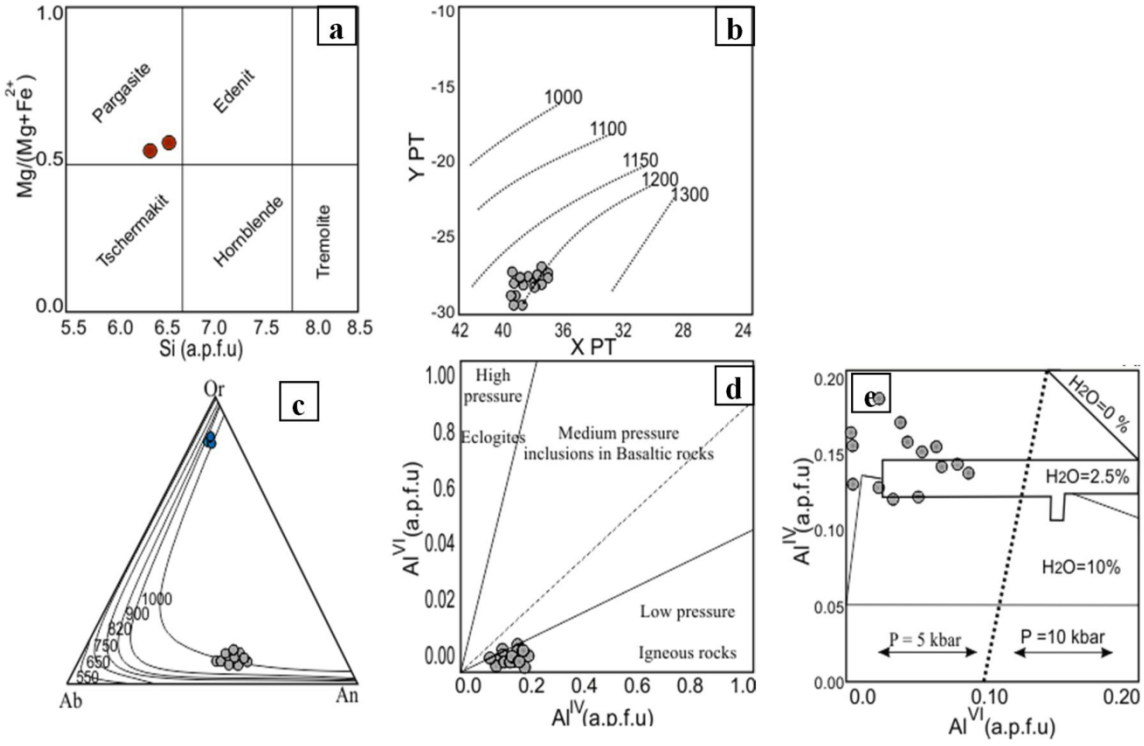

Fig 5. a) In the diagram of Leake et al. (1997), amphibole microcrystals have pargasite composition. b) The diagram XPT vs. YPT from Soesoo (1997) estimates formation temperature of clinopyroxenes about 1200 ˚C (In this diagram from Soesoo (1997) XPT and YPT are equivalent to following formulas: Xp_T= 0.446 SiO_2 + 0.187 TiO_2- 0.404 Al_2O_3 + 0.346 FeO_{TOTAL}- 0.052 MnO + 0.309 MgO + 0.431 CaO -0.446 Na_2O. Yp_T= -0.369 SiO_2 + 0.535 TiO_2-0.317 Al_2O_3 + 0.323 FeO_{TOTAL}+ 0.235 MnO-0.516 MgO-0.167 CaO - 0.153 Na_2O). c) Feldspar triangular thermometry diagram (Kroll et al. 1993) shows all feldspars are formed between 900 and 1000 $^{\circ C}$. d) Clinopyroxene barometry diagram (Helz 1976) all samples placed in low-pressure field. e) Al^{VI} vs. Al^{IV} diagram (Aoki and Shiba 1973) shows water content of studied rocks magma were about ~2.5 to less than 10%.

7. Evaluation of Oxygen Fugacity

Oxygen fugacity plays an important role in changing of the liquids temperature, melt and crystals composition, magmatic processes controlling, crystallization sequence and types of crystallized minerals (France et al. 2010; Botcharnikov et al. 2005). Using Al^{IV} +Na vs. Al^{IV} + 2Ti + Cr diagram, which depend on the content of ferric iron in pyroxenes, to determine the oxygen fugacity of the system. The diagram set based on the aluminum content that has been balanced in the tetrahedral position with Cr^{3+} in the octahedral position. The Fe^{3+} in pyroxenes can be whit 3-valence elements such as Al^{VI}, Ti and Cr in the octahedral position. In the other hand Fe^{3+} in pyroxenes depends on the amount of Al^{VI}, which means it hinge on the aluminum balance in tetrahedral and octahedral position (France et al. 2010).

In the studied clinopyroxenes the M1 site dominantly occupied by Mg (0.61–0.79) atom per formula unit (a.p.f.u.) with minor content of Fe^{2+} (0.03–0.23 a.p.f.u.). The M2 site is almost fully occupied by Ca (0.83- 0.89 a.p.f.u), while Na (0.03-0.05 a.p.f.u), Mn (~0.01 a.p.f.u.) and Mg contents in M2 site (0.06–0.12 a.p.f.u.) are low (Table 2). In all clinopyroxenes, Al atom in T Site is enough for filling the absence of Si^{4+} in the tetrahedral sites (0.10- 018 a.p.f.u) (Fig 6a).

Figure 6b shows that the pyroxenes which crystalized at high oxygen fugacity, is situated above the line of Fe^{3+}. Furthermore, Papike and Cameron, (1976) have been noted that more distance of the samples from the Fe^{3+} line are indicating more oxygen fugacity in their host magma. In this diagram, studied pyroxenes are located above the Fe^{3+} line (Fig 6c).

France et al (2010) by using of Fe^{3+}/ Fe^{2+} ratio in coexist plagioclase and clinopyroxene crystals according to formula (1) Calculated Log fO_2 of the host magma. Also according to the formula (2), they calculated buffering values (ΔNNO).

(1) log fO_2=ΔFMQ + (82.75 + 0:00484T−30681 / T−24.45 log T + 940P / T−0.02P)

(2) ΔNNO = log fO_2−(12.78−25073 /T−1.1 log T + 450P /T + 0:025P)

According to equation 1 and 2 the measured fugacity and buffering for studied rocks are 8.38-11.51 and 3.09-0.23 respectively. High content of buffering in the clinopyroxene mineral chemistry has been prevented widespread chemical changes in the studied Cpx crystals. Moreover according to Smith and Anderson's (1995), the Fe# = (Fe/Fe+Mg) content in the amphibole between 0.0 to 0.6 indicated high content of oxygen fugacity and 0.6 to 0.8 contents indicate medium oxygen fugacity. If Fe# content is between 0.8 to 1.0 indicated low oxygen fugacity. Also in the Table 3, the Fe# content of analyzed amphibole crystals is 0.41 to 0.47 that imply high oxygen fugacity. High amounts of Fe and Mg in biotite minerals depend on oxygen fugacity during Magma cooling process (Wones and Eugster 1965). In the high fO_2 condition, biotite crystals are Fe-rich and Magnetite co-exists with biotite. In the low fO_2 crystallization condition, biotite will be in Fe content and magnetite is rarely exist (Castro and Stephen 1992). Biotite crystals show high content of MgO (12.6 - 14.47) and MgO# (0.45- 0.47) and FeO (14.56-16.56), FeO# (0.53-0.55), this imply their formation in a high oxygen fugacity condition. According to Figure 3c and data represented in Table 3, all analyzed opaque minerals are magnetite and confirm high oxygen fugacity of the magma.

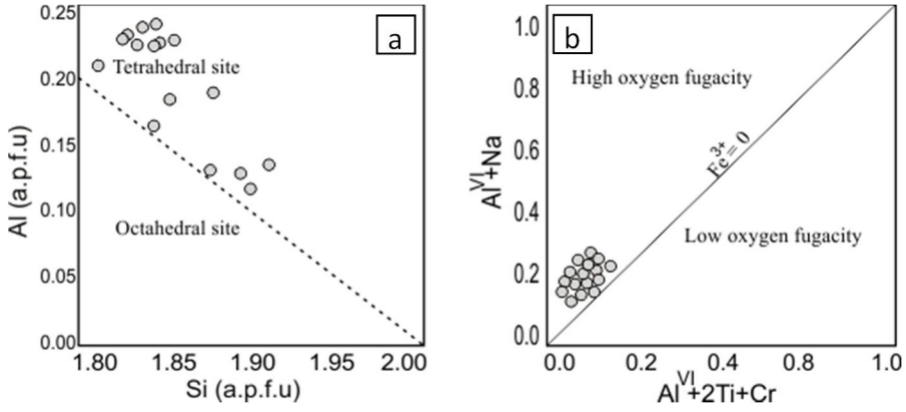

Fig 6. a) Si (a.p.f.u) versus Al (a.p.f.u) diagram from Leterrier et al (1982), show all sample with shares of aluminum in tetrahedral site. b)Estimation of oxygen fugacity in pyroxenes according to Diagram the Al^{VI}+2Ti+Cr versus Al^{IV}+Na, (Schweitzer et al. 1979) shows all the samples fall in the upper side of Fe^{3+} line.

8. Magma Series and Tectonomagmatic Setting

Pyroxenes composition intensely depends on the chemical composition and tectonic setting of the host magma. This fact can widely be used to determine magma series, and geological setting of the basic rocks (Kushiro 1960; Schweitzer et al. 1979; Hout et al. 2002).

In the clinopyroxene crystals, Ca, Ti, Al and Na elements show high frequency in the crystallization formula and the magma alkalinity degree can be determined by using these elements (LeBas 1962; Leterrier et al. 1982). In Ca+ Na vs. Ti diagram (Leterrier et al. 1982), all samples show alkaline nature (Fig 7a). Also in Al_2O_3 vs. SiO_2 diagram (LeBas 1962), mainly samples are placed in the alkaline field however, some of them located in the sub alkaline field (Fig 7b). Alkaline amphiboles have K_2O>1 while sub-alkaline type represent lower K_2O content (Tiepolo et al. 2011). Studied amphiboles in the TiO_2 vs. K_2O diagram (Fig 7c) fall in the alkaline field. Amphiboles from magma related to subduction settings (S-Amph) have lower contents of Na_2O and TiO_2 in comparison with amphiboles (I-amphibole) of magmas from interpolate tectonic settings (Caltorti et al. 2007). Amphiboles from studied rocks with SiO_2 values of 43.60 – 45.16 and Na_2O values of 1.12 – 1.67 have been evaluated in the tectonic setting diagram and they fall in the S-amphibole type part that imply host magma originated in a subduction-related tectonic setting (Fig 7d).

Also in diagram Ca vs. Ti+Cr (Leterrier et al. 1982) (Fig 7e) and TiO_2 +Cr_2O_3 (Wt. %) versus Al_2O_3 (Wt. %) tectonic setting diagram (Hout et al. 2002) all sample placed in BABB field (Fig 7f). According to the data about clinopyroxene minerals chemistry in Pushtasar basaltic rocks with Ti (a.p.f.u) from 0.018 to 0.056, Ca+Na (a.p.f.u) from 0.78 to 0.87, SiO_2 (wt.%) from 50.04 to 52.1, Al_2O_3 (wt.%) from 3.07 to 4.6 and TiO_2+Cr_2O_3 from 0.65 to 2.03, the all Pushtasar basaltic clinopyroxene ranges are shown in diagrams (Fig 7a, b and f). According to clinopyroxene minerals chemistry, Pushtasar basaltic rocks are placed in the alkaline and BAB field (Fig 7a, b and f).

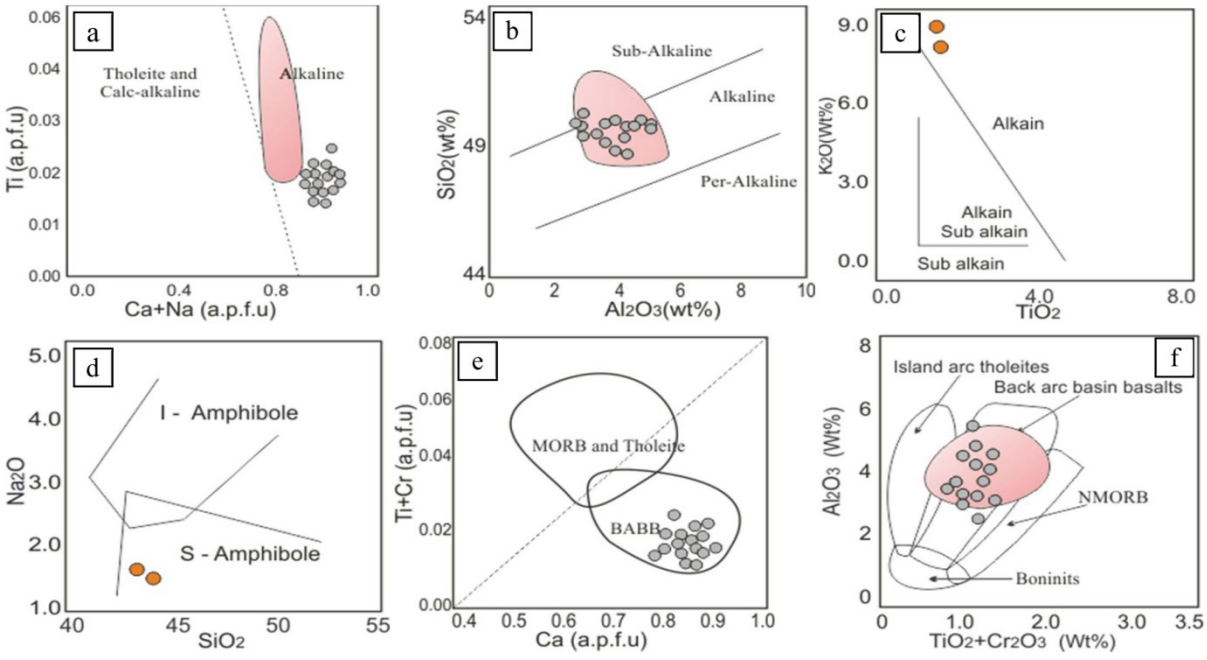

Fig 7. a) Diagram Ca+Na (a.p.f.u) vs. Ti (a.p.f.u) (Leterrier et al. 1982) shows all the samples are in the alkaline field. b) Diagram Al_2O_3 (Wt. %) vs. SiO_2 (Wt. %) (Leterrier et al. 1982) shows all the samples in Alkaline and some of them are in sub alkaline field. c) K_2O vs. TiO_2 diagram (Molina et al. 2009); studied samples are in the alkaline field. d) Na_2O vs. SiO_2 diagram for studied amphiboles (Coltorti et al. 2007). e) Ti+Cr (a.p.f.u) vs.Ca (a.p.f.u) Diagram (Leterrier et al. 1982). f) Al_2O_3 (Wt. %) vs. TiO_2+Cr_2O_3 (Wt. %) Diagram (Hout et al. 2002) all samples are in Back-arc basin basalts (BABB) field. The range determined in the diagrams (Fig 4a, b, and c) is relevant to mineral chemistry in the Pushtasar basaltic rocks (Mobashergermi et al. 2015).

9. Comparison of studied basalts with Pushtasar basaltic rocks

The currently studied basaltic rocks in some local places have pillow structure and they rarely have olivine minerals. Also microlithic groundmass of these rocks includes hydrous mineral such as mica, amphibole, alkali feldspars (Sanidine) and volcanic glass. This rock shows low alteration. However, according to Mobashergermi et al. (2015) and Mobashergermi (2013), the Poshtasar basaltic rocks in northern part of the study area is rich in olivine minerals, groundmass generally have glassy and less hydrous and potassic minerals such as mica and sanidine. Also, high alteration is shows with sericitic plagioclase and production of secondary chlorite minerals.

According to labradoritic plagioclase and diopsidic clinopyroxene thermometry in the studied basalt, estimated crystallization temperature varies between 1000˚C to ~1050 ˚C and 1106˚C to ~1200 ˚C but in the Pushtasar basaltic rocks labradoritic plagioclase and diopsidic to augite compound clinopyroxene thermometry are show in range 950˚C and ~1000 ˚C.

In terms of the general pressure estimation, the both clinopyroxenes compounds basaltic rock in this study and basaltic prisms assemblages of Pushtasar show the formations in pressure of about 5 kbar to diagram Aoki and Shiba (1973).

The clinopyroxenes in the basaltic prisms assemblages of Pushtasar rocks show crystallized at high oxygen fugacity (Mobashergermi 2013). Also this study basaltic rocks show crystallized at high oxygen fugacity.

According to the chemistry of studied clinopyroxene minerals, the both basaltic magmatisms have shown the host magma alkaline nature. The amounts of Na_2O and K_2O in the study basaltic clinopyroxenes are 0.57 and less than 0.01 respectively and in clinopyroxenes of Pushtasar basaltic prisms are ~0.10 and less than 0.08 respectively. Also clinopyroxenes in these study basaltic rocks have Mg#= 76 to 93 variable but clinopyroxenes in Pushtasar basaltic rocks have Mg#~ 69 to 75 variables. The clinopyroxene mineral composition of studied rocks and Pushtasar basaltic rocks indicate that they have been formed in a back-arc basin environment.

10. Conclusion

Basaltic Eocene rocks are outcropped in the southwest of Germi. These basaltic rocks contain plagioclase with labradorite composition, clinopyroxene with diopside composition phenocrysts in grandmas of feldspar, biotites, amphibole and volcanic glass. Clinopyroxenes crystals represent normal zoning and they have been formed in low-pressure crystallization condition and from basic magma with ~2.5% to less than 10% water content. Chemistry of clinopyroxene crystals showed that they have been crystallized at 1106$^{\circ C}$ - 1200$^{\circ C}$ and high oxygen fugacity (-8.38-11.51). These results confirmed by biotite and amphibole data. Also, thermometry of plagioclase and sanidine indicate a temperature of about 900$^{\circ C}$ - 1000$^{\circ C}$. According to chemistry of studied minerals, the host basaltic magma show alkaline nature and have been originated in a back arc basin tectonic setting. The result of this research shows the similarity of these basaltic rocks mineral chemistry characteristics and that of Pushtasar basaltic rocks.

Acknowledgments

The authors would like to thank the anonymous reviewers for their valuable comments and suggestions to improve the quality of the paper.

References

Abdel Rahman AM (1994) Nature of biotites from alkaline, calc-alkaline and per aluminous magmas. *Journal of Petrology* 35: 525-541.

Aghazadeh M, Castro A, Badrzadeh Z, Vogt K (2011) Post-collisional polycyclic plutonism from the Zagros hinterland. The Shaivar-Dagh plutonic complex Alborz belt, Iran. *Geological Magazine* 148: 980-1008.

Aghazadeh M, Castro A, Omrani N R, Emami M H, Moinevaziri H, Badrzadeh Z (2010) The gabbro (shoshonitic)-monzonite-granodiorite association of Khankandi pluton, Alborz mountains, NW Iran. *Journal of Asian Earth Sciences* 38: 199-219.

Anderson LJ (1996) Status of thermobarometry in granitic batholiths. *Geological Society of America Special Papers* 315: 125-138.

Aoki K, Shiba I (1973) Pyroxenes from lherzolite inclusions of Itinomegata-Gata, Japan. *Lithos* 6: 41-51.

Avanzinelli R, Bindi L, Menchetti S, Conticelli S (2004) Crystallization and genesis of per alkaline magmas from Pantelleria volcano, Italy: an integrated petrological and crystal-chemical. *Lithos* 73(1–2): 41-69.

Babakhani AR, KhanNazer H (1997) Geological Quadrangle Map and repot 1:100000 Lahrud, No.5567. *Geological Survey of Iran* (in Persian).

Beane RE (1974) Biotite stability in the porphyry copper environment. *Economic Geology* 69: 241-256.

Beccaluva L, Macciotta G, Piccardo GB, Zeda O (1989) Clinopyroxene composition of ophiolite basalts as petrogenetic indicator. *Chemical Geology* 77: 165-182.

Berberian F, Berberian M (1981) Tectono-plutonic episodes in Iran. American Geophysical Union. *Geodynamics Series* 3: 5-32.

Berman R (1988) Internally consistent thermodynamic data for minerals in the system Na_2O-K_2O-CaO-MgO-FeO-Fe_2O_3- Al_2O_3-SiO_2-TiO_2-H_2O-CO_2. *Journal of Petrology* 29: 445-522.

Bindi L, Cellai D, Melluso L, Conticelli S, Morra V, Menchetti S (1999) Crystal chemistry of clinopyroxene from alkaline undersaturated rocks of the Monte Vulture volcano, Italy. *Lithos* 46: 259-274.

Botcharnikov R, Koepke J, Holtz F, McCammon C, Wilke M (2005) The effect of water activity on the oxidation and structural state of Fe in a Ferro-basaltic melt. *Geochimica et Cosmochimica Acta* 69: 5071-5085.

Brunet MF, Korotaevb MV, Ershovb AV, Nikishinb AM (2003) The South Caspian Basin: a review of its evolution from subsidence modeling. *Sedimentary Geology* 156: 119-148.

Castro A, Aghazadeh M, Badrzadeh Z, Chichorro M (2013) Late Eocene-Oligocene post-collisional monzonitic intrusions from the Alborz magmatic belt, NW Iran. An example of monzonite magma generation from a metasomatized mantle source. *Lithos* 181: 109-127.

Castro A, Stephen WE (1992) Amphibole rich clots in calcalkalin granitic rocks and their enclaves. *The Canadian Mineralogist* 30: 1093-1112.

Coltorti M, Bonadiman C, Faccini B, Grégoire M, O`Reilly S Y, Powell W (2007) Amphiboles from suprasubduction and intraplate lithospheric mantle. *Lithos* 99: 68-84.

Deer WA, Howie R A, Zussman J (1992) An Introduction to the rock-forming minerals. *Longman* 528p.

France L, Ildefonse B, Koepke J, Bech F (2010) A new method to estimate the oxidation state of basaltic series from microprobe analyses. *Journal of Volcanology and Geothermal Research* 189: 340-346.

France L, Koepke J, Ildefonse B, Cichy SB, Deschamps F (2010) Hydrous Partial Melting in the Sheeted Dike Complex at Fast Spreading Ridges: Experimental and Natural Observations. *Contributions to Mineralogy and Petrology* 160: 683-704.

Gasparik T (1984) Two-pyroxene thermobarometry with new experimental data in the system CaO-MgO, Al_2O_3-SiO_2. *Contributions to Mineralogy and Petrology* 87: 87-97.

Gioncada A, Hauser N, Matteini M, Mazzuolir M, Omarini R (2006) Mingling and mixing features in basaltic andesites of the eastern Cordillera (central Andes, 24S): a petrographic and microanalytical study. *Periodico di Mineralogia* 75(3): 127-140.

Hammarstrom A, Jane M, Zen EA (1986) Aluminum in hornblende: An empirical igneous geobarometer. *American Mineralogist* 71: 1297-1313.

Helz RT (1976) Phase relations of basalts in their melting ranges at P_{H2O}= 5 kbar: Part melt compositions. *Journal of Petrology* 17: 139-193.

Hendry DA, Chivas AR, Long JVP, Reed SJB (1985) Chemical differences between minerals from mineralizing and barren intrusions from some North American prophyry copper deposits. *Contributions to Mineralogy and Petrology* 89: 317-329.

Huot F, Hébert R, Varfalvy V, Beaudoin G, Wang C, Liu Z, Cotten J, Dostal J (2002) The Beimarang mélange (southern Tibet) brings additional constraints in assessing the origin, metamorphic evolution and obduction processes of the Yarlung Zangbo ophiolite. *Journal of Asian Earth Sciences* 21(3): 307-322.

Kroll H, Evangelakakis C, Voll G (1993) Two-feldspar geothermometery: A review and revision for slowly cooled rocks. *Contributions to Mineralogy and Petrology* 114: 510-518.

Kuscu GG, Floyd P (2001) Mineral compositional and textural evidence for magma mingling in the Saraykent volcanic rocks. *Lithos* 56: 207-230.

Kushiro I (1960) Si-Al Relation in clinopyroxenes from igneous rocks. *American Journal of Science* 258: 548-554.

LeBass NJ (1962) The role of aluminous in igneous clinopyroxenes and plagioclase with relation to their parentage. *American Journal of earth Science* 260: 267 - 88.

Leterrier J, Maurry RC, Thonon P, Girard D, Marchal M (1982) Clinopyroxene composition as a method of identification of the magmatic affinites of paleo-volcanic series. *Earth and Planetary Science Letters* 59: 139-154.

Manoli S, Molin G (1988) Crystallographic procedures in the study of experimental rocks: X-ray single-crystal structure refinement of clinopyroxene from Lunar 74275 high-pressure experimental basalt. *Mineralogy and petrology* 39: 187-200.

Masson F, Djamour Y, Van Gorp S, Chéry J, Tavakoli F, Nankali H, Vernant P (2006) Extension in NW Iran driven by the motion of the south Caspian basin. *Earth and Planetary Science Letters* 252: 180-188.

Mobashergermi M (2013) Petrology, petrography and geochemical studies of basaltic rocks in Southwest of Germi (Ardabil province). MSc thesis, Department of Geology, University of Tabriz, Tabriz, Iran (in Persian).

Mobashergermi M, Akbari Z, Jamshedibadr M (2015) Geochemistry, petrogeneses and origin magmatic evolution in the olivine gabbro dikes in Southwest of Germi city. *Journal of Petrology* 6(20): 65-86 (in Persian).

Mobashergermi M, Zaraisahameh, R, Jahangeri A, (2015) Petrography and mineral chemistry of basaltic Prisms in south of Germi city, Pushtasar axis (South talesh). *Journal of new findings in geology practical* 6(20): 65-86 (in Persian).

Molina J, Scarrow J, Montero PG, Bea F (2009) High-Ti amphibole as a petrogenetic indicator of magma chemistry: evidence for mildly alkalic-hybrid melts during evolution of Variscan basic-ultrabasic magmatism of central Iberia. *Contribution to Mineralogy and Petrology* 158: 69-98.

Morimoto N, Fabrise J, Ferguson A, Ginzburg IV, Ross M, Seifert FA, Zussman J, Akoi KI, Gottardi G (1988) Nomenclature of pyroxenes. *Mineralogical Magazine* 52: 535 -55.

Papike JJ, Cameron M (1976) Crystal chemistry of silicate minerals of geophysical interest. *Reviews of Geophysics* 14: 37-80.

Perugini D, Poli G, Valentini L (2005) strange attractors in plagioclase oscillatory zoning petrological implications. *Contributions to Mineralogy and Petrology* 149: 482-497.

Princivalle F, Tirone M, Comin-Chiaramonti P (2000) Clinopyroxenes from metasomatized spinel-peridotite mantle xenoliths from Nemby (Paraguay): crystal chemistry and petrological implications. *Mineralogy and Petrology* 70: 25-35.

Schmidt MW (1992) Amphibole composition in tonalite as a function of pressure: an experimental calibration of the Al in hornblende barometer, *Contributions to mineralogy and Petrology* 110: 304 -310.

Schweitzer E, Papike J, Bence A (1979) Statistical analysis of clinopyroxenes from deep-sea basalts. *American Mineralogist* 64: 501-513.

Soesoo A (1997) A multivariate statistical analysis of clinopyroxene composition: empirical coordinates for the crystallization PT-estimations. *Geological Society of Sweden. Geologiska Föreningen* 119: 55-60.

Stein E, Dietl C (2001) Hornblende thermobarometry of granitoids from the Central Odenwald (Germany) and their implications for the geotectonic development of the Odenwald. *Mineralogy and Petrology* 72: 185–207.

Taylor W, Nimis J (2000) Thermometry clinopyroxene in the Hawaii basalt. *Mineralogy* 21: 25-36.

Vynhal CR, McSween HY, Speer JA (1991) Hornblende chemistry in southern Appalachian granitoids: Implications for aluminum hornblende thermobarometry and magmatic epidote stability. *American Mineralogist* 76: 176-188.

Whitney D L, Evans B.W. (2010) Abbreviations for names of rock-forming minerals. *American Mineralogist*, 95: 185–187.

Wones DR, Eugster HP (1965) Stability of biotite: experiment, theory and application. *American Mineralogist* 50: 1228-1272.

Wones DR, Gilbert MC (1982) Amphiboles in the igneous environment. *Mineralogical Society of America Reviews in Mineralogy* 9: 355-390.

Yoder HS, Tilley GE (1962) Origion of basalt magmas: an experimental study of natural and synthetic rock systems. *Journal of Petrology* 3: 348-532.

Zhu Y, Ogasawara Y (2004) Clinopyroxene phenocrysts (with green salite cores) in, trachybasalts: implications for two magma chambers under the Kokchetav UHP massif, North Kazakhstan. *Journal of Asian Earth Sciences* 22: 517-527.